Ultrasonic surface wave parameters monitoring using 3D vibrometry and ellipsometry for local material characterization

A. Bouzzit, Andrés Arciniegas, L. Martinez, S. Serfaty, Nicolas Wilkie-Chancellier

forum acusticum 2023

ULTRASONIC SURFACE WAVE PARAMETERS MONITORING USING 3D VIBROMETRY AND ELLIPSOMETRY FOR LOCAL MATERIAL CHARACTERIZATION

A. Bouzzit[1]* **A. Arciniegas**[1] **L. Martinez**[1]
S. Serfaty[1] **N. Wilkie-Chancellier**[1]
[1] Laboratoire Systèmes et Applications des Technologies de l'Information et de l'Energie (SATIE - UMR CNRS 8029), CY Cergy-Paris Université, France

ABSTRACT

Rayleigh wave is widely used in non-destructive testing and evaluation, the three-dimensional vibrations inspection highlights the bivariate nature of these waves and their elliptic motion. The links between this motion and the material properties are well established, however, theoretical expressions are very sensitive to the measurement errors and the purity of the surface wave. If the classical processing often uses independently the two components of the wave, it seems more complete to process the two components together using the adequate bivariant filters.
This work presents the monitoring of the 3D propagation of ultrasonic Rayleigh waves and the signal processing dedicated to the identification of their characteristic parameters. It is particularly focused on the wave ellipticity, i.e. the horizontal to vertical component ratio (*H/V*-ratio). This phenomenon is studied analytically, numerically and experimentally. Over a scanned area, the local mechanical parameters are estimated using time signals extracted from each single point.
The obtained results for Aluminum show a good agreement between the analytical, numerical and experimental studies of Rayleigh wave ellipticity. Moreover, these H/V ratios are consistent with the theoretical values found in literature. This method is also applied on simulation data to study orthotropic materials (wood/bone), obtaining promising results.

Keywords: *Ellipsometry, 3D vibrometer, Rayleigh waves, Material characterization.*

*__Corresponding author__: aziz.bouzzit@cyu.fr

1. INTRODUCTION

Nondestructive testing of cultural heritage can be challenging due to the delicate nature of the objects and materials. Surface acoustic waves (SAW) like Rayleigh waves [1] are useful in material investigation as they propagate on the material's surface, making them accessible. Rayleigh waves have low attenuation and can cover a relatively large distance before being attenuated, making them ideal for acoustic contactless nondestructive testing. A 3D laser vibrometer can be used to extract the three components of deformation generated by the SAW, highlighting the elliptic nature of the motion of the Rayleigh wave [2]. This motion can be characterized by the ellipticity ($\chi=H/V$) and orientation of the ellipse (θ), both are related to the mechanical properties of the material.
Geophysicists used directional geophones to measure the three components of the vibration of surface waves These measurements allowed them to be the first to use the ellipticity of Rayleigh waves to characterize soil. The *H/V* spectral ratio was introduced by Nogoshi and Igarashi in 1971[3], and later popularized by Nakamura [4], [5], who highlighted a correlation between the *H/V* spectral ratio and the fundamental resonance frequency of the observed geological site. The simplicity and efficiency of this method made it popular in geophysical studies, and Molnar et al. have listed its applications and advancements [6].
Malischewsky developed models for H/V ratio as a function of mechanical properties [7]. Meanwhile, laser vibrometry and material characterization advanced with the technique of Aussel and Monchalin for elastic constant determination [8] and method of Orta et al for identifying orthotropic elastic stiffness [9]. Staszewski et al. provided an overview of laser doppler vibrometry for structural health monitoring [10].

In 2006, Bayon proposed a contactless method for estimating the dynamic elastic constant of isotropic materials using a 2D laser vibrometer and the *H/V* ratio model by Malischewsky. The Young's modulus (E) and Poisson's ratio (v) can be estimated from the *H/V* ratio and Rayleigh wave velocity with an accuracy of 0.82% for E and 4.4% for v [2]. However, accurate results require extracting a pure Rayleigh wave to avoid errors introduced by the presence of other wave types.

In practical cases, extracted signals may contain different types of waves and noises that interfere with the spectra of the Rayleigh wave, leading to errors in the *H/V* estimation. The bivariate signal processing frame provides a solution to this issue by estimating the eigenpolarization of a bivariate signal, considering both components of the signal at the same time [11]. This method is more effective than the traditional *H/V* spectral ratio method, which is sensitive to noise and added undesired waves in the signal. The Hermitian linear time invariant filters used in bivariate signal processing can accurately estimate the dominant polarization of the Rayleigh wave, despite the presence of other waves and noises in the extracted signal.

This paper presents the theoretical background of the *H/V* value for an isotropic half-space and its sensitivity to measurement errors. It also introduces the Hermitian filters method for estimating the eigenpolarization of a bivariate signal and validates it using theoretical and finite element simulation signals. The experimental setup used for signal extraction and the results obtained through the Hermitian filters method are presented and discussed.

2. THEORATICAL BACKGROUND

2.1 The theoretical expression of *H/V*

Rayleigh waves are a kind of surface wave that propagate along the free surface of a body. The disturbance caused by these waves is confined to a thin surface layer whose depth is proportional to its wavelength. When the medium is homogeneous and isotropic, the particle motion of Rayleigh waves near the surface is retrograde and elliptical. The major normal axis of the ellipse is perpendicular to the free surface, which means that the vibration plane contains the direction of propagation and is perpendicular to the surface [12]. The velocity of Rayleigh waves, as well as the phase velocities of bulk waves longitudinal and shear, are related by this mathematical equation [2], [13], [14]

$$R^3-8(R-1)(R-2-2\kappa^2)=0 \quad (1)$$

where $R = V_R^2/V_T^2$ and $\kappa = V_T/V_L$, if V_L, V_T and V_R are respectively the longitudinal, transverval and Rayleigh wave velocities.

The theoretical expression of the ratio between the in-plane and the out-of-plane deformations, is expressed as function of R by the formula [7]:

$$\chi_R = H/V = 2\frac{\sqrt{1-R}}{2-R} \quad (2)$$

In the case of an isotropic half-space, the mechanical properties of the material, Young modulus (E), Poisson ratio (v) and the density (ρ) are related to the phase velocities of Rayleigh longitudinal and shear waves and the theoretical expression are well defined. Based on this relation the inverse problem relating the mechanical properties with the *H/V* ratio and V_R is established [2], [15]. Measurement errors made on *H/V* will affect the estimated values for the mechanical properties. The study of the relative error committed on the estimation of *H/V* as function of the relative error on R showed that, for a 10% relative error on R the relative deviation on the estimation of *H/V* is around 20% and can reach up to 87% depending on the material. These results highlight the importance of measuring *H/V* with minimum errors.

2.2 Hermitian filtering for the estimation of the ellipse parameters

As a Rayleigh wave travels in the sagittal plane, only the normal and tangent components in the direction of propagation change. This unique characteristic makes the extracted signals in the sagittal plane being classified as bivariant signals. The bivariant signals framework offers valuable tools for processing signals with two components. Unlike the *H/V* spectral ratio method, the advantage of this framework is that the two components are treated simultaneously rather than separately.

Hermitian filters are linear time invariant filters that operate on the frequency domain by performing a Hermitian transform on each frequency of the input bivariant signal, modifying both the power and polarization properties. The diattenuation axis of the filter represents the polarization at which the gain is maximum, known as the eigenpolarization [11]. By adjusting the polarization parameter, the filter can detect if the input signal matches the Hermitian filter's polarization. A bank of these filters is needed to detect the range of polarization values in the input signal.

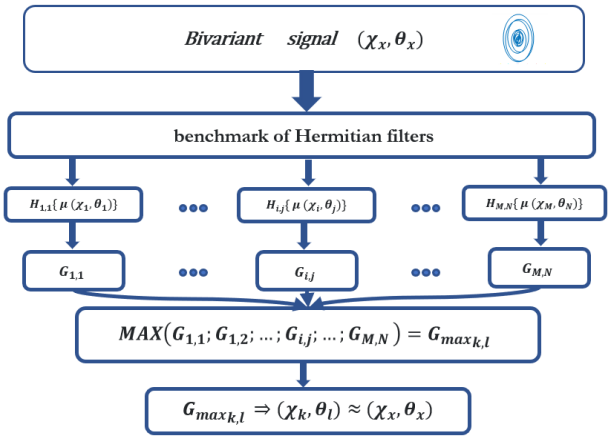

Figure 1: The information flow followed to estimate the ellipticity parameters.

The process of determining the polarization value is depicted in Figure (1) : ellipticity χ and orientation θ. Initially, the bivariant signal undergoes filtering with various eigenpolarization values. Then, the gain at the output of each filter is determined, and the polarization parameters of the filter with the highest gain are retrieved. These parameters correspond to the dominant polarization of the input signal.

Ellipticity values range from $\chi \in [-1;1]$ and orientation values range from $\theta \in [-\pi/2; \pi/2]$. Discretizing the value ranges with small steps yields precise polarization estimation, but at the cost of longer computation time. In Figure (1), the subscripts i,j represent the indices of discretized values for χ and θ , and M and N are the total number of values for χ and θ , respectively. Plotting gain values as a function of χ and θ allows for better visualization of gain variation and the maximum position.

This approach allows for better estimation of polarization parameters in the presence of Rayleigh wave propagation and different types of noise. The method is tested on theoretical, finite elements simulation, and experimental signals.

3. VALIDATION

This section evaluates the ability of Hermitian filters to estimate polarization parameters of a bivariant signal from a propagating Rayleigh wave on the sagittal plane, using different signal types. The signals include a synthetic monochromatic signal with fixed polarization parameters, a signal extracted from a finite element simulation of a Rayleigh wave on the surface of an aluminum block, and a signal monitored using a 3D vibrometer measuring a Rayleigh wave on the surface of an aluminum block.

3.1 Synthetic signal

For aluminum the values of longitudinal and shear waves velocity are respectively V_T=6374m/s and V_L=3111 m/s. By using equations (1) and (2), the values of the ellipticity and orientation are estimated to be χ=0.626 and θ=π/2 rad. A bivariant signal is synthesized based on this values (Figure (2)) and injected to the bank of Hermitian filters.

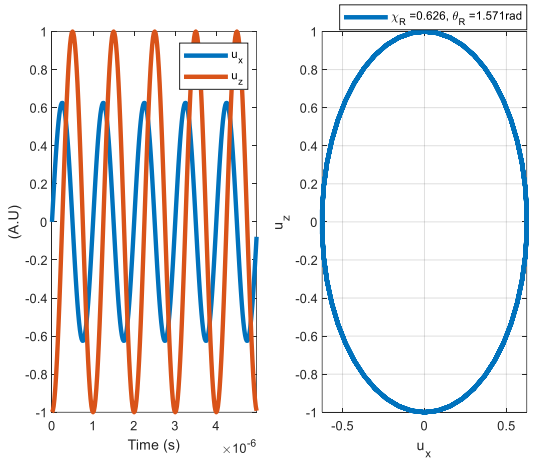

Figure 2: Synthetic bivariant signal of a monochromatic Rayleigh wave.

In Figure (2) the two components of a Rayleigh wave in the sagittal plane (u_x,u_z) are plotted on the left. The variation of u_z as function of u_x is plotted on the right, highlighting the elliptic shape.

The variation of the gain at the output of each filter is then presented as function of χ and θ (Figure (3)). For this synthetic signal, the maximum gain corresponds to χ_{synth}= 0.625 and θ_{synth} = 1.571 rad, the relative error on the estimation of the parameters are Err_χ=0.16% and Err_θ=0%. These results reflect the performance of the proposed method in the case of a perfect monochromatic harmonic bivariant signal. In the next subsection the performance is tested on a more realistic signal from numerical simulations.

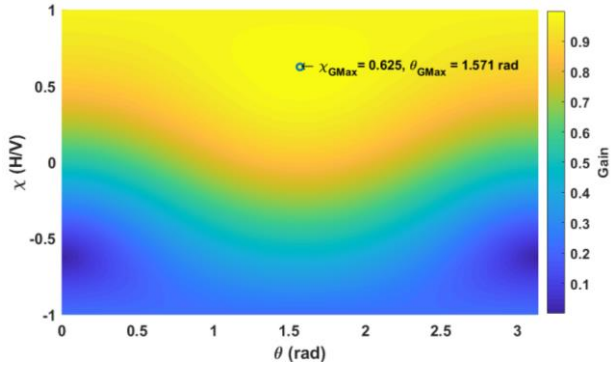

Figure 3: The gain as function of χ and θ for the synthetic signal.

3.2 Simulation signal

The numerical simulation allow us to generate more realistic signals, extracted from Rayleigh waves propagating on material with different properties and shapes.

The propagation of SAW on an aluminum block is simulated with the same properties used in the synthetic case (V_L=6374m/s, V_T=3111 m/s. and a density of ρ =2730 kg/m^3) by a finite element method allowing time and space discretization of the propagation. The excitation is a 5 cycles tone burst with central frequency f_0=0.75MHz. The simulation is carried out using a 3D model, the position of extraction is chosen on the sagittal plane of the propagation, as in this plane only two components of the deformation change, the normal and the tangent in direction of propagation of the wave.

A time dependent solver is used to study the propagation of the SAW, the time step between two iterations is fixed to $dt=1/(10\ f_0)$. The geometry of the material is discretized using a triangular mesh where the maximum element size is fixed to $L_{Max}=V_T/(10\ f_0)$.

Figure (4) illustrates the calculated deformation of the Rayleigh wave at the instant t_i=3.7μs , also the position of the excitation and the extraction are indicated along with the sagittal plane of the wave.

The extracted bivariant signal is shown in Figure (5) in a time signal of the two components and in a plot of u_z as function of u_x. As the excitation, the recovered signal is a tone burst with central frequency of f_0, compared to the synthetic case this signal is a more realistic and will also us to test the proposed method. The simulation signal is passed though the benchmark of filters and the results are shown in Figure (6).

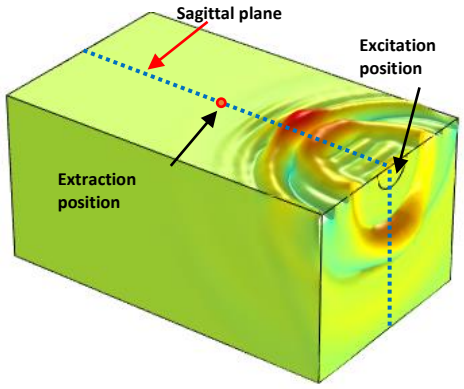

Figure 4: Simulation results : displacement at instant t_i=3.7μs .

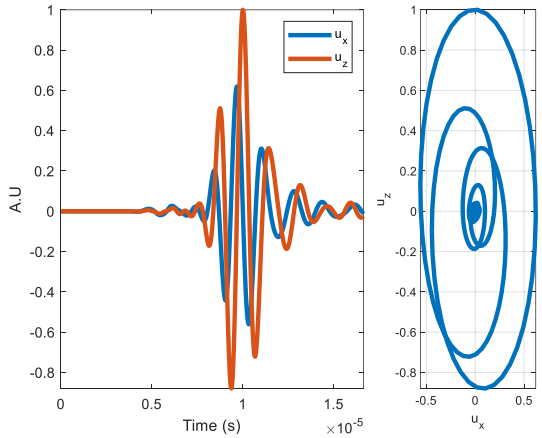

Figure 5: The bivariant signal extracted from the simulation.

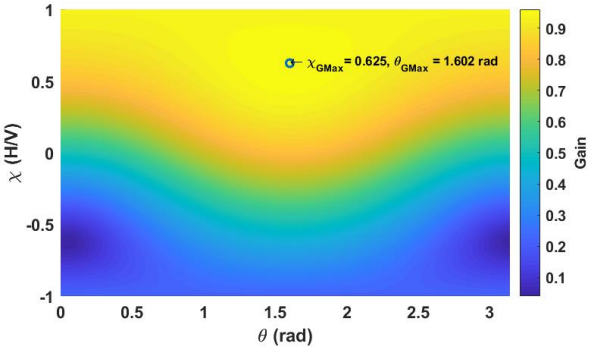

Figure 6: The gain as function of χ and θ for the simulated signal.

For the simulated signal the maximum gain is found for the parameters χ_{simul}= *0.625* and θ_{simul} =*1.602* rad. Based on the V_T and V_L the theoretical values of χ and θ are the same as the synthetic case.
The relative error on the estimation of the parameter are Err_χ=*0.16%* and Err_θ=*1.9%*. For the ellipticity, the error is the same as in the synthetic case, meaning that the performance of the benchmark of filters is the same for a monochromatic and tone burst excitation. But the error on θ is rather high compared to synthetic case. Despite that, the method is able to estimate with good accuracy *(<2%)* the polarization parameters of the wave.

3.3 Experimental signal

In order to complete the validation process, it is necessary to test the proposed method on actual experimental signals obtained from a propagating Rayleigh wave. To achieve this, a block of aluminum measuring 20×12.5×10 cm³ is utilized to support the wave propagation. The velocities of the Rayleigh and shear waves on the block are respectively measured to be V_R=*2888m/s*, V_T=*3092 m/s*. The surface wave is generated using a f_c=*1 MHz* shear wave transducer mounted on the side of the block. This last applied a force tangent to surface, this will generate a Rayleigh wave on the adjacent face [16] and the signal is extracted on the sagittal plane of the wave using the experimental set up shown in Figure (7).

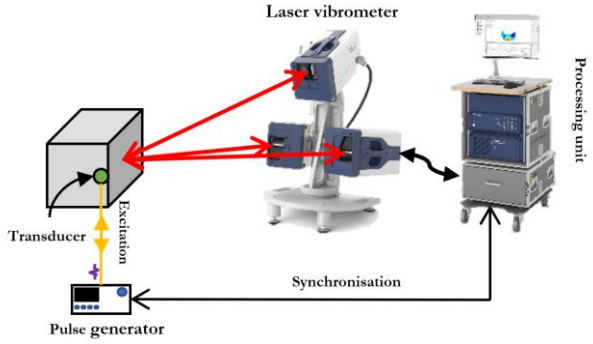

Figure 7 : Experimental set-up.

The vibrometer is positioned to face the side on which the wave is propagating. The pulse generator JSR Ultrasonics DPR300 generates the excitation and synchronization signals. The Laser Vibrometer Polytec ® PSV 500-3D-V extracts the time signals, and can measure the three components of displacement (u_x,u_y,u_z) with frequencies up to *25MHz*. The extraction can be performed on a single point or a grid of predefined points, this will allow us to estimate the mechanical properties. of the material located on the extraction position. This aspect highlights the locality of extracted information, where information is related to the position of the extraction.
The bivariant signal extracted on the surface of the block is shown in Figure (8)

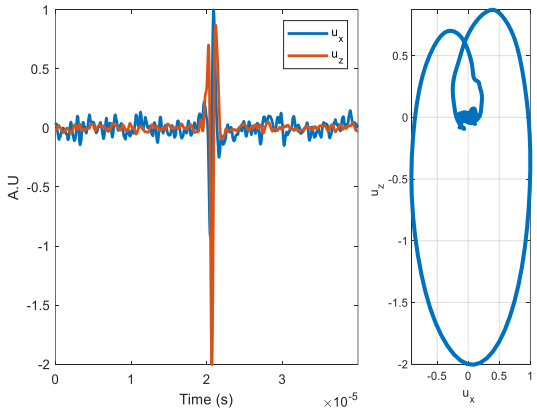

Figure 8: Bivariant signal measured using the experimental setup.

Figure (8) depicts the experimental case signal, which exhibits noise that was not present in the previous two types of signals. This signal was subjected to the Hermitian filter benchmark, and the resulting gain variation with respect to χ and θ is shown in the figure.

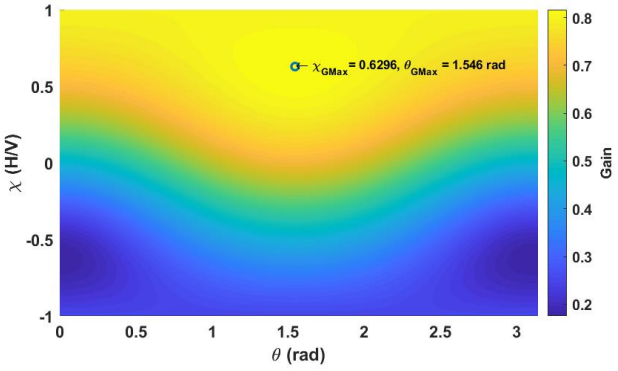

Figure 9: The gain as function of χ and θ for the experimental signal.

From the V_T and V_R for values for the aluminum block, and by means of equation (2), the theoretical value of the elliptic parameters are χ_{theo} = 0.639 and θ_{theo}=*π/2 rad*. Our method estimates these two parameters for the experimental case to be χ_{exp} = 0.629 and θ_{theo}= *1.546 rad*. The relative error

between the theoretical values and the estimated experimental values are $Err_{\chi}=1.4\%$ and $Err_{\theta}=1.6\%$.
Despite the presence of noise in the signal obtained from the experimental setup, the Hermitian filter benchmark successfully estimates the polarization parameters of the propagating of Rayleigh wave with very small relative error. The same experimental signal is analyzed using the *H/V* spectral ratio method, the results are illustrated on Figure (10).

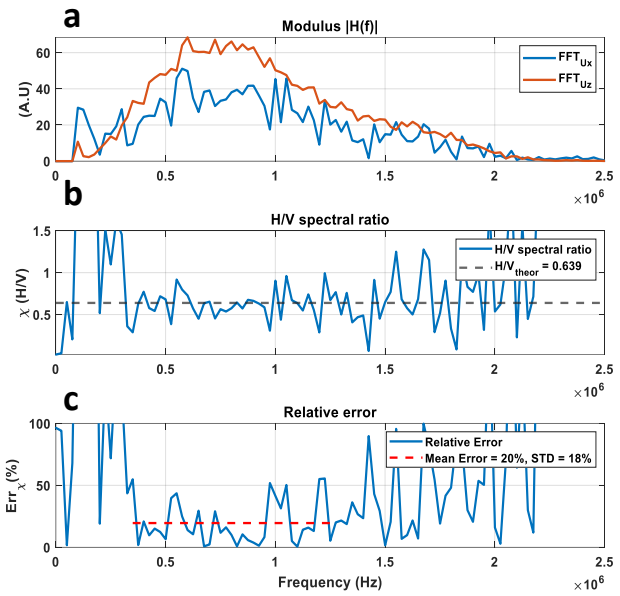

Figure 10: **a**-Fourier transform of the two components of signal, **b**-*H/V* spectral ratio, **c**-the error relative to the theoretical value.

The Fourier transform of the two components of the experimental bivariant signal are presented in Figure (10- a) for frequencies ranging from *0* to *2.5 MHz*. The two components have relatively the same content in terms of frequency, the bandwidth is ranging roughly from *0.3* to *1.3 MHz*. In this interval, oscillations can also be seen, resulting from the noise present in the signal and its interference within the bandwidth of propagating wave.
The *H/V* spectral ratio method consists on calculating the ratio between the FFT of the two components of the bivariant signal (U_z/U_x). The results of this operation is plotted on Figure(10- b), a line representing the theoretical value of χ is also plotted.
Two mean intervals are to be noticed, in the bandwidth, the values of *H/V* vary with $\sigma=0.17$ standard deviation around the theoretical one, and out of the bandwidth, where the values show big deviations. As a result, one will only be interested in the values within the bandwidth. The relative error between the estimated *H/V* spectral value and the theoretical value is plotted in Figure (10- c) : the error is once more relatively low for the frequencies within the bandwidth. The mean value of the relative error over this interval is *20%* with *18%* standard deviation. This value is bigger than the one estimated by the benchmark of Hermitian filters ($Err_{\chi}=1.4\%$). This result shows the capacity of the proposed method to estimate the parameters of polarization of bivariant Rayleigh wave, as the estimation is based on the eigenpolarization of the signal rather than the simple ratio between the spectra of the two components.

4. APPLICATION ON DIFFERENT MATERIALS

The following section employs the benchmark of filters to estimate the polarization of simulated Rayleigh waves that travel through various materials (such as wood and bones). The purpose is to examine how the ellipticity of the wave changes based on different factors such as the type of wood or the postmortem interval of the bone. The propagation of waves in the sagittal plane of different materials is simulated using a 2D finite element method with a time-dependent solver, the parameters of the simulation are the same as those used in subsection 3.2.

4.1 Wood: two different species.

Wood is commonly found in cultural heritage objects, and it's essential to identify the species of wood used for restoration purposes. In this section, simulations of Rayleigh waves were conducted on two classes of wood (softwood: *DOUGLAS FIR* and hardwood: *SWEETGUM*) with different rigidities to observe if the $\chi=H/V$ parameter varies. The material properties of the two species of wood used in the simulation, the stiffness tensor and the density of orthotropic wood with *12%* humidity (dry state), are extracted from the Wood handbook [17], and simulations were limited to the RL plane (direction of wood fibers) to save time.
Figure (11) illustrates the bivariant signal extracted from the simulation of Rayleigh wave propagation on the two species of wood. The results obtained show that the ellipticity values for *DOUGLAS FIR* ($\chi_{DOUGLAS\text{-}FIR}=0.024$) and *SWEETGUM* ($\chi_{SWEETGUM}=0.103$) are lower compared to aluminum ($\chi_{Al}=0.625$). This can be attributed to the orthotropic nature of wood, which makes it more resistant to deformation in certain directions than others [18]. In the case of the simulated woods, the deformation is easier in the normal direction than in the tangent direction, as seen in the

significant difference in amplitude between the u_z and u_x components of deformation. The χ values also differ between the two types of wood, with hardwood having a higher value by a factor of 5 compared to softwood. Therefore, χ could be a useful parameter in distinguishing between the two species of wood.

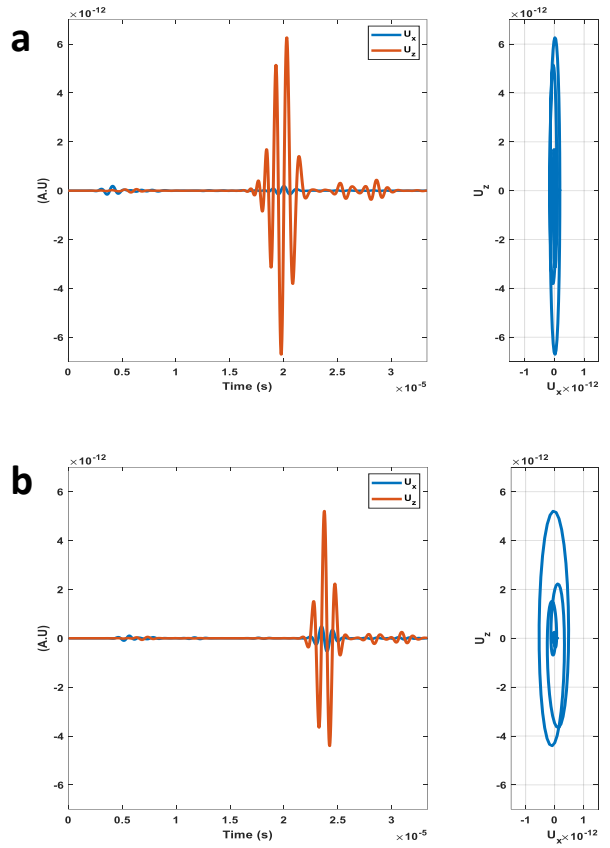

Figure 11 : Extracted bivariant signal from simulation: a-DOUGLAS FIR, b-SWEETGUM.

4.2 Bones: different post mortem intervals (PMI)

Accurately estimating the postmortem interval (PMI) of bones is crucial in the fields of archaeology and criminology. In this study, simulations were conducted to analyze the propagation of Rayleigh waves on bones with varying PMIs, and their polarization properties were extracted using the Hermitian filter benchmark. The simulations were carried out using the rigidity tensor of bones with different PMIs, and the average values of these tensors can be found in A. Angermuller's thesis (2021) [19]. For the same PMI the values on the tensor varies from an individual to another due to the variation in the growth conditions. For this, only the mean values of the tensors are used and the variation is represented with the error bars in the results. Four simulations were performed for PMIs of 3 years, 13 years, 50 years, and archaeological remains older than 500 years. The results of the simulations are summarized in Figure (12).

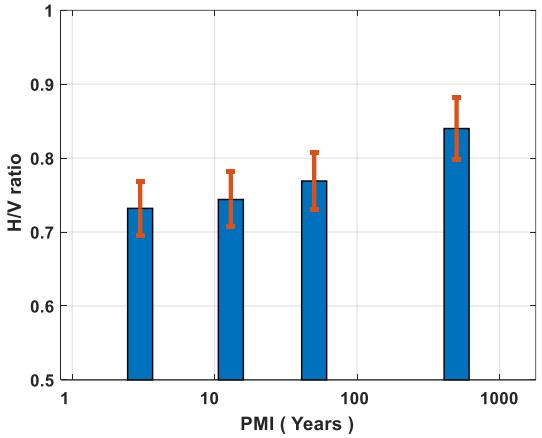

Figure 12 : χ=H/V variation as function of the PMI of the bone.

The mean values of χ for different bones range from *0.74* to *0.84 (0.74< χ_{bone}<0.84)*, and it can be observed that mean value of χ increases as a function of postmortem interval. The increasing trend of χ suggests that the rigidity of bones may increase with PMI, which is supported by the observation of χ increasing from softwood to hardwood. For a given material, the ellipticity of Rayleigh waves also increases with rigidity.

We have demonstrated that the ellipticity of Rayleigh waves can serve as a characterization parameter to distinguish between hardwood and softwood, and provide an indication of bone rigidity (related to PMI). However, these results are preliminary and based only on simulated signals, and experimental validation is necessary. Furthermore, a theoretical model comparison would enable the extraction of additional useful information, beyond simply comparing values.

5. CONCLUSION

This work presents a nondestructive evaluation method for cultural heritage material using surface acoustic waves such as Rayleigh waves. A 3D laser vibrometer measures the three components of the deformation generated by the propagating wave, and the ellipticity and orientation of the elliptical motion characterize the motion. A method based

on Hermitian filters extracts the eigenpolarization of a bivariant signal to estimate the polarization properties of Rayleigh waves. Results from simulations and experiments show the capacity of χ to distinguish between different types of wood and characterize bones with different PMI. Future work will focus on the theoretical model for the orthotropic case to extract more useful information about the mechanical constants of the wood or bones, followed by experimental validation.

6. ACKNOWLEDGMENTS

This work is supported and funded by CY Cergy Paris University.

7. REFERENCES

[1] Lord Rayleigh, "*Lord Rayleigh_On Waves Propagated along the Plane Surface of an Elastic Solid*_1885," London Mathematical society, 1885, doi: https://doi.org/10.1112/plms/s1-17.1.4.

[2] A. Bayón, F. Gascón, and F. J. Nieves, "*Estimation of dynamic elastic constants from the amplitude and velocity of Rayleigh waves*," J Acoust Soc Am, vol. 117, no. 6, pp. 3469–3477, Jun. 2005, doi: 10.1121/1.1898663.

[3] M. NOGOSHI, "*On the amplitude characteristics of microtremor, Part II*," Journal of the seismological society of Japan, vol. 24, pp. 26–40, 1971.

[4] Y. Nakamura and others, "*Clear identification of fundamental idea of Nakamura's technique and its applications*," in Proceedings of the 12th world conference on earthquake engineering, 2000, pp. 1–8.

[5] Y. Nakamura, "*A method for dynamic characteristics estimation of subsurface using microtremor on the ground surface*," Railway Technical Research Institute, Quarterly Reports, vol. 30, no. 1, 1989.

[6] S. Molnar et al., "*A review of the microtremor horizontal-to-vertical spectral ratio (MHVSR) method*," J Seismol, vol. 26, no. 4, pp. 653–685, Aug. 2022, doi: 10.1007/s10950-021-10062-9.

[7] P. G. Malischewsky and F. Scherbaum, "*Love's formula and H/V-ratio (ellipticity) of Rayleigh waves*," Wave Motion, vol. 40, no. 1, pp. 57–67, 2004, doi: 10.1016/j.wavemoti.2003.12.015.

[8] J.-D. Aussel and J.-P. Monchalin, "*Precision laser-ultrasonic velocity measurement and elastic constant determination*," Ultrasonics, vol. 27, no. 3, pp. 165–177, May 1989, doi: 10.1016/0041-624X(89)90059-0.

[9] A. H. Orta, M. Kersemans, and K. Van Den Abeele, "*On the Identification of Orthotropic Elastic Stiffness Using 3D Guided Wavefield Data*," Sensors, vol. 22, no. 14, p. 5314, Jul. 2022, doi: 10.3390/s22145314.

[10] W. J. Staszewski, R. bin Jenal, A. Klepka, M. Szwedo, and T. Uhl, "*A Review of Laser Doppler Vibrometry for Structural Health Monitoring Applications*," Key Eng Mater, vol. 518, pp. 1–15, Jul. 2012, doi: 10.4028/www.scientific.net/KEM.518.1.

[11] J. Flamant, P. Chainais, and N. Le Bihan, "*A complete framework for linear filtering of bivariate signals*," Feb. 2018, doi: 10.1109/TSP.2018.2855659.

[12] I. A. Viktorov, "*Rayleigh and Lamb Waves: Physical Theory and Applications*," 1967.

[13] D. Nkemzi, "*A new formula for the velocity of Rayleigh waves*," Wave Motion, vol. 26, no. 2, pp. 199–205, Sep. 1997, doi: 10.1016/S0165-2125(97)00004-8.

[14] *Theory of Elasticity. Elsevier*, 1986. doi: 10.1016/C2009-0-25521-8.

[15] T. V.-B. Daniel Royer, *Ondes élastiques dans les solides 1: Propagation*, vol. Volume 1. 2021.

[16] L. Adler and P. B. Nagy, "*Measurements of acoustic surface waves on fluid-filled porous rocks*," J Geophys Res Solid Earth, vol. 99, no. B9, pp. 17863–17869, Sep. 1994, doi: 10.1029/94JB01557.

[17] R. J. Ross and F. P. Laboratory. USDA Forest Service., "*Wood handbook : wood as an engineering material*," 2010. doi: 10.2737/FPL-GTR-190.

[18] V. Bucur and F. Rocaboy, "*Surface wave propagation in wood: prospective method for the determination of wood off-diagonal terms of stiffness matrix*," Ultrasonics, vol. 26, no. 6, pp. 344–347, Nov. 1988, doi: 10.1016/0041-624X(88)90033-9.

[19] A. Angermuller, "*Etudes de signatures ultrasonores de l'os en vue d'une datation post mortem*," CY Cergy Paris Université, 2021.